Structures 26 (2020) 901–914

Contents lists available at ScienceDirect

Structures

journal homepage: www.elsevier.com/locate/structures

Nonlinear seismic soil-structure interaction analysis of nuclear reactor building considering the effect of earthquake frequency content

Dong Van Nguyen[a], Dookie Kim[a,*], Duan Duy Nguyen[b]

[a] Civil and Environmental Engineering, Kongju National University, Cheonan-daero, Seobuk-gu, Cheonan, Chungcheongnam-do 31080, Republic of Korea
[b] Department of Civil Engineering, Vinh University, Vinh 461010, Viet Nam

ARTICLE INFO

Keywords:
Reactor building
Nuclear power plant
Three-dimensional nonlinear analysis
Soil-structure interaction
Earthquake frequency content
Time domain

ABSTRACT

A three-dimensional nonlinear soil-structure interaction analysis is simulated in time domain in order to evaluate the behavior of a nuclear reactor building under different earthquake motions. The effects of earthquake frequency content and soil-structure interaction are taken into account by using three different ground motions and four different soil types. Viscous boundary and free-field column are used to absorb propagating waves and consider the free-field motion in the soil medium, respectively. Analysis of three cases are carried out: (i) linear analysis, (ii) nonlinear analysis with the bonded contact between superstructure and soil medium, and (iii) nonlinear analysis with the sliding contact between superstructure and soil medium. The results obtained from the time domain are validated by using a code in the frequency domain, and a good agreement is found between two methods. By changing the soil properties and ground motions, some comparisons of the nuclear reactor responses are made. It is concluded that both of soil-structure interaction and earthquake frequency content are highly sensitive to the behavior of nuclear reactor building under seismic loading. Also, this research leads to some new findings that are useful for practical applications while considering the soil-structure interaction and earthquake frequency content in nuclear structures.

1. Introduction

Soil-structure interaction is an important factor for dynamic loadings, especially earthquake in many fields of practical applications. Safety-critical structures, such as high-rise buildings, long-span bridges, concrete dams, and nuclear power plants need to be carefully evaluated with the consideration of soil-structure interaction. Seismic analyses of nuclear power plant structures considering soil-structure interaction were studied numerously. In the study of Zhou and Wei [1], a nuclear power plant model was employed to examine the influence of different soil properties on seismic response of an isolated nuclear power plant in frequency domain. Kumar et al. [2] focused on investigating the seismic response of a nuclear containment structure considering the nonlinear Winkler model for the soil–foundation interface. Abell et al. [3] assumed that the incoming wave field produced by an earthquake, is unidimensional and vertically propagating. Then, seismic soil-structure interaction analyses of nuclear power plants were implemented by using explicit modeling of sources, seismic wave propagation, site, and structure. Bolisetti et al. [4] presented the assessment of the soil-structure interaction codes of LS-DYNA and SASSI for nuclear structures. The soil-structure interaction analysis can be solved in the frequency domain or time domain. And, each approach has its own advantages and disadvantages. For nuclear power plants, the problem of soil-structure interaction is usually analyzed in the frequency domain. A system for analysis of soil-structure interaction (SASSI) is one of the most commonly used codes for the soil-structure interaction analysis in the frequency domain [5]. The algorithm of SASSI is based on the principle of superposition. For that reason, SASSI can only solve linear analyses. In order to increase the accuracy of the soil-structure interaction analysis, the nonlinear behavior of the system should be considered. To that end, analyses in the time domain cannot be avoided. In this study, a time domain code, ABAQUS [6], is used to implement nonlinear soil-structure interaction analyses.

The presence of spurious waves at the boundaries of the soil model leads to inaccurate results in the soil-structure interaction analysis. The simplest way to dissipate the spurious waves is to make a large soil medium. However, the use of a large soil medium is not computational cost-effective and sufficient. Artificial boundary condition is known as an advanced solution to solve the soil boundary condition problem. By using the artificial boundary conditions to absorb the spurious waves, the soil medium can be truncated to a smaller domain. Then, the soil-structure interaction system with artificial boundary conditions is

* Corresponding author.
E-mail address: kim2kie@kongju.ac.kr (D. Kim).

https://doi.org/10.1016/j.istruc.2020.05.013
Received 22 December 2019; Received in revised form 15 March 2020; Accepted 8 May 2020

analyzed more cost-effectively and accurately. There have been many kinds of artificial boundary conditions proposed, such as viscous boundary [7], perfectly matched layers [8], perfectly matched discrete layers [9], perfectly matched discrete layers with analytical wave-lengths [10–12], and infinite elements [13]. Viscous boundary is known as one of the first absorbing boundary conditions and it is still commonly used because of its simplicity and acceptable results for practical applications. In this study, viscous boundary is applied along the boundaries of the soil model.

In seismic soil-structure interaction analyses, one of the important issues is the consideration of the free-field motion under earthquakes. For a truncated soil medium, the free-field motion is not maintained as the original one, i.e. infinite soil medium. One of the solutions for that is to calculate the free-field responses first. Then, the free-field motion is applied along the boundaries of the soil model [14,15]. The procedure is applied for all the nodes of the fine-element model of the soil medium. This solution is not easy for practical application. For the sake of simplicity, in this study, free-field columns are placed next to the soil medium to consider the free-field motion. This method is based on the study of Zienkiewicz et al. [16]. The principle of the method is to use the free-field columns to convert the free-field motions to the free-field tractions at the boundaries of the soil medium.

Besides soil-structure interaction, the earthquake frequency content is another important characteristic of the seismic analysis. There are many parameters used to evaluate the frequency content of an earthquake motion, such as predominant period, mean period, power spectrum intensity, and the ratio between peak ground acceleration (PGA) which is expressed in units of g to peak ground velocity (PGV) expressed in units of m/s [17–19]. Among those, PGA/PGV ratio is a simple and useful parameter to provide the information of earthquake frequency. Usually, earthquake motions are divided into three types based on the ratio of PGA/PGV [20]: (i) high frequency content when $PGA/PGV > 1.2$, (ii) intermediate frequency content when $1.2 \geq PGA/PGV \geq 0.8$, and (iii) low frequency content when $PGA/PGV < 0.8$.

There are some studies on the effect of earthquake frequency content on different structures considering soil-structure interaction, such as storage tank [21] and retaining wall [22]. However, to the knowledge of the authors, the specific study of the effect of the earthquake frequency content for the seismic soil-structure interaction problem of nuclear reactor buildings with the nonlinear analysis in three-dimensional space is still limited. Due to the importance of the problem, a study is necessary to investigate the soil-structure interaction and earthquake frequency content effects on the behavior of nuclear reactor buildings in an accurate analysis, i.e. three-dimensional nonlinear analysis. In this study, four soil types with different properties and three earthquake records with different frequency contents are used to evaluate the responses of a nuclear reactor building. The study leads to some new findings that are useful for practical applications in terms of soil-structure interaction and earthquake frequency content consideration in nuclear structures.

2. Numerical simulation

2.1. Structural modeling

In the present study, the reactor building of the APR1400 nuclear power plant is considered. A superstructure system including the containment building, internal structure, and basement is founded on a soil medium (Fig. 1(a) and (b)). The heights of the containment building and internal structure from the basemat are $78m$ and $34.5m$, respectively. And, the depth of the soil medium is $30m$. The basement is a circular solid with the radius of $25m$ and thickness of $3m$. The containment building and internal structure are modeled by using stick models with lumped masses for the sake of simplicity and computational cost effectiveness (Fig. 1(c)). Lumped-mass stick model has been widely used for nuclear power plant structure [23–26]. To consider the reality of the connection between concrete walls of superstructure and basemat, rigid links are used to connect the stick model and basemat. Properties of the structural models of the containment building and internal structure are given in Tables 1 and 2, respectively.

The concrete material is used for the superstructure. The material properties are presented in Table 3. In this study, the structural system is analyzed by using ABAQUS, a finite element analysis program. Both linear and nonlinear analyses are provided in ABAQUS to fully evaluate the behavior of the nuclear reactor building. Concrete Damage Plasticity (CDP) model, which is available in ABAQUS, is selected to represent the nonlinear material of concrete. CDP has been known as a proper constitutive model to simulate the nonlinear behavior of concrete material under dynamic loadings. Two failure mechanisms of concrete are assumed in CDP model: tensile cracking and compressive crushing [6].

The finite element model of the superstructure is shown in Fig. 2. Beam elements (B33) in ABAQUS are used for the containment building and internal structure (Fig. 3(a)). And, there are two kinds of solid elements applied for the basemat: C3D8 with 8 nodes and C3D6 with 6 nodes (Fig. 3(b) and (c)).

Material damping is independent of frequency. And, it is used to form the complex stiffness of structural models. For that reason, material damping is implemented easily in the frequency domain. However, in the time domain, material damping needs to be converted to Rayleigh damping. To form Rayleigh damping, the mass-proportional (α) and stiffness-proportional (β) coefficients are calculated from selected natural frequencies (ω_m and ω_n of modes m and n) and the damping ratio (ξ). The values of α and β are defined as follows [27]:

$$\alpha = \xi\frac{2\omega_m\omega_n}{\omega_m + \omega_n} \tag{1}$$

$$\beta = \xi\frac{2}{\omega_m + \omega_n} \tag{2}$$

For the superstructure, the first and second natural frequencies are selected to determine the values of α and β coefficients. The modal analysis of the superstructure gives the first and second natural frequencies values of $\omega_1 = 35.1(rad/s)$ and $\omega_2 = 131.9(rad/s)$, respectively. From Eqs. (1) and (2) with the material damping of 5%, the mass-proportional and stiffness-proportional coefficients are $\alpha = 2.772$ and $\beta = 0.0006$, respectively.

2.2. Soil modeling

The present study considers the soil-structure interaction with the soil medium founded on the bedrock at the depth of $H = 30m$ (Fig. 4). From the research of Rayhani and El Naggar [28], this bedrock depth is reasonable because most of amplification is in the first $30m$ of the soil medium. In this study, the reactor building with surface foundation is considered.

The soil medium is truncated into a small domain with the dimensions of $200mx200m$ (Fig. 4(b) and (c)). Then, to absorb the propagating waves, absorbing boundary conditions are assigned at the lateral boundaries of the soil medium. Here, viscous dashpots are used for this purpose (Fig. 4(b) and (c)). And, the bedrock is simulated by rigid boundary. The coefficients of dashpots are defined as follows [7]:

$$C_n = \rho c_p \tag{3}$$

$$C_s = \rho c_s \tag{4}$$

where C_n and C_s are the normal and shear coefficients of dashpot; ρ, c_p, and c_s are the density, primary wave, and shear wave velocities, respectively.

In this study, free-field columns are used to consider the free-field motion (Fig. 4). The principle of the free-field columns is to convert from the free-field motions to free-field tractions at soil medium

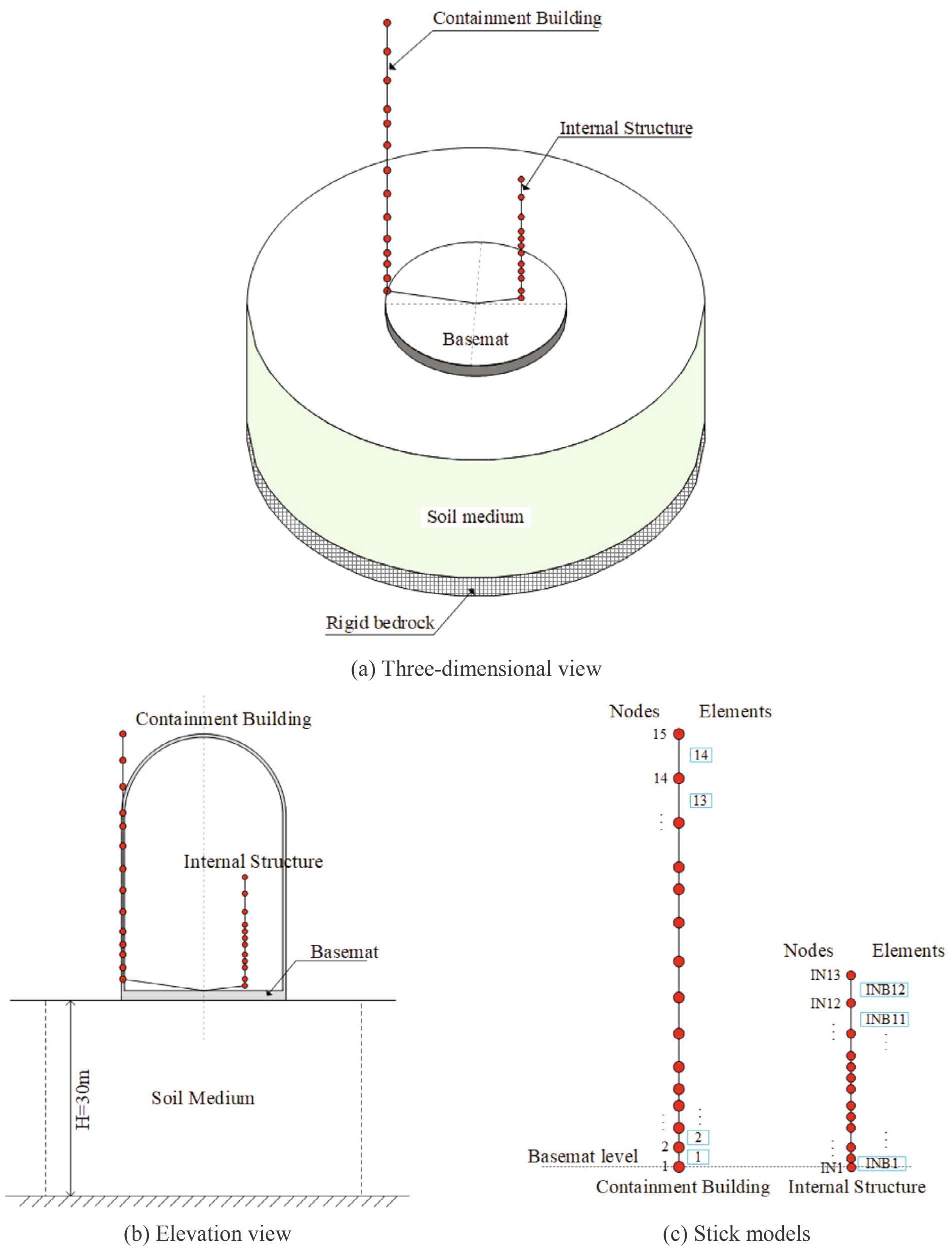

Fig. 1. Soil-structure system.

Table 1
Properties of containment building.

Node	Height from the base (m)	Lumped mass (ton)	Element	Connecting nodes	Area (m^2)	Shear area (m^2)	Moment of inertia (m^4)	Torsional inertial (m^4)
1	0.0	853.7	–	–	–	–	–	–
2	3.5	1633.1	1	1 to 2	202.9	101.5	56299.8	112634.2
3	7.0	1818.4	2	2 to 3	202.9	101.5	56299.8	112634.2
4	11.0	1856.3	3	3 to 4	202.9	101.5	56299.8	112634.2
5	14.0	1671.0	4	4 to 5	202.9	101.5	56299.8	112634.2
6	18.0	2301.4	5	5 to 6	202.9	101.5	56299.8	112634.2
7	24.0	3080.8	6	6 to 7	202.9	101.5	56299.8	112634.2
8	30.5	3266.1	7	7 to 8	202.9	101.5	56299.8	112634.2
9	37.0	3118.7	8	8 to 9	202.9	101.5	56299.8	112634.2
10	44.0	3044.3	9	9 to 10	202.9	101.5	56299.8	112634.2
11	50.0	3695.2	10	10 to 11	202.9	101.5	56299.8	112634.2
12	54.0	2745.1	11	11 to 12	202.9	101.5	56299.8	112634.2
13	62.0	3486.5	12	12 to 13	179.8	89.9	47591.2	95199.7
14	70.0	3452.9	13	13 to 14	179.8	89.9	35861.7	71732.0
15	78.0	1449.2	14	14 to 15	166.1	83.0	12825.6	25651.3

Table 2
Properties of internal structure.

Node	Height from the base (m)	Lumped mass (ton)	Element	Connecting nodes	Area (m^2)	Shear area (m^2)	Moment of inertia (m^4)	Torsional inertial (m^4)
IN1	0.0	1806.1	–	–	–	–	–	–
IN2	1.5	3348.0	INB1	IN1 to IN2	833.2	662.8	79896.9	164989.7
IN3	3.5	7810.8	INB2	IN2 to IN3	884.0	704.3	81942.5	167389.1
IN4	7.0	5135.4	INB3	IN3 to IN4	857.9	684.0	80710.1	165957.8
IN5	9.0	2678.3	INB4	IN4 to IN5	313.8	221.8	21253.4	37753.4
IN6	11.0	2905.6	INB5	IN5 to IN6	254.6	171.1	19443.0	35811.7
IN7	14.0	2911.2	INB6	IN6 to IN7	221.9	144.3	19384.0	35233.9
IN8	16.0	3486.0	INB7	IN7 to IN8	261.4	175.9	20166.3	36571.3
IN9	18.0	789.5	INB8	IN8 to IN9	202.8	130.8	18524.1	34566.9
IN10	20.0	2595.2	INB9	IN9 to IN10	202.8	130.8	18524.1	34566.9
IN11	24.0	2507.4	INB10	IN10 to IN11	202.7	130.8	18524.1	34566.9
IN12	29.5	2665.1	INB11	IN11 to IN12	103.2	94.9	4666.7	7888.6
IN13	34.5	798.1	INB12	IN12 to IN13	97.9	92.3	4642.6	7840.4

Table 3
Material properties of concrete.

Young's modulus (kN/m^2)	Poisson's ratio	Mass density (t/m^3)	Material damping (%)	Dilation angle (degrees)	Compressive strength (kN/m^2)	Tensile strength (kN/m^2)
$3.045x10^7$	0.17	2.4	5	30	32,000	3200

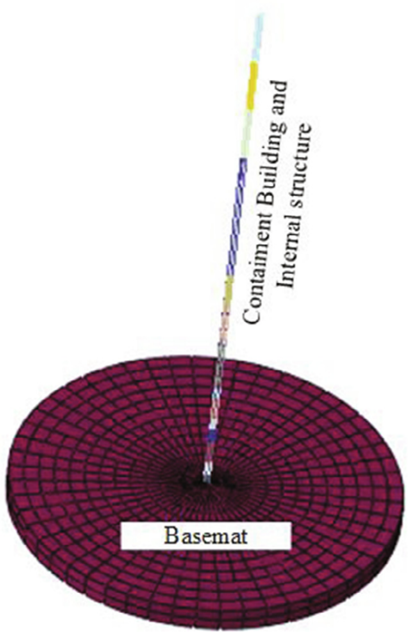

Fig. 2. Finite element model of the superstructure.

boundaries with following equations:

$$\sigma_n = \rho c_p(\dot{u}_n^i - \dot{u}_n^f) + \sigma_n^f \quad (5)$$

$$\sigma_s = \rho c_s(\dot{u}_s^i - \dot{u}_s^f) + \sigma_s^f \quad (6)$$

In which σ_n and σ_s are the normal and shear free-field tractions; $\dot{u}_n^i$ and $\dot{u}_s^i$ are the normal and shear velocities; $\dot{u}_n^f$ and $\dot{u}_s^f$ are the normal and shear velocities evaluated in the free-field; σ_n^f and σ_s^f are the normal and shear tractions contributed from free-field.

The effect of the soil-structure interaction is investigated by considering four types of soil as presented in Table 4. The soil types and their properties are selected based on the recommendation from previous studies [29,30]. In the table, $S1$, $S2$, $S3$, and $S4$ vary from very stiff soil ($S1$) to soft soil ($S4$). The nonlinear material of soil is evaluated by using Drucker-Prager model, which is available in ABAQUS. According to ABAQUS documentation, the value of dilation angle is defined the same as the friction angle and the value of flow stress ratio is set to 1. In this study, Drucker Prager hardening behavior is shear type with the yield stress equal to cohesion yield value. The Drucker-Prager is pressure-dependent model and widely used in geotechnical applications for soil and rock. It is known as a smooth version of Mohr-Coulomb model. The effectiveness and accuracy of the Drucker-Prager have been proved by many studies [31–33].

Rayleigh damping coefficients of the soil medium are obtained from Eqs. (1) and (2). The frequencies used to calculate the mass-proportional and stiffness-proportional coefficients are selected from the first and second natural frequencies of the soil medium. The values of natural frequencies of the soil medium is obtained as following equation [34]:

$$\omega_n = \pi(2n-1)\frac{c_s}{2H} \quad (7)$$

where n is the mode number; c_s and H are the shear wave velocity and the depth of the soil medium, respectively.

The values of Rayleigh damping coefficients are given in Table 5.

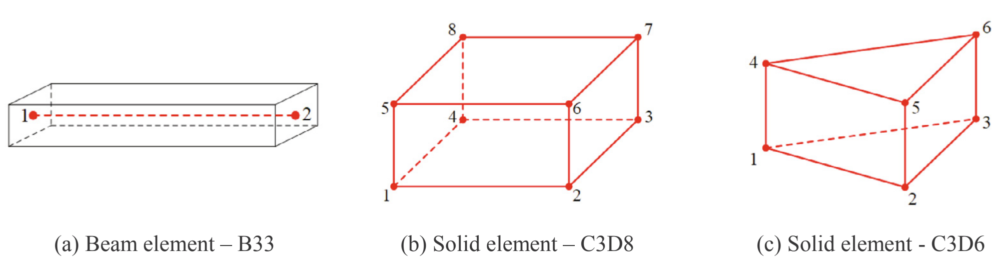

Fig. 3. Elements used for finite element model.

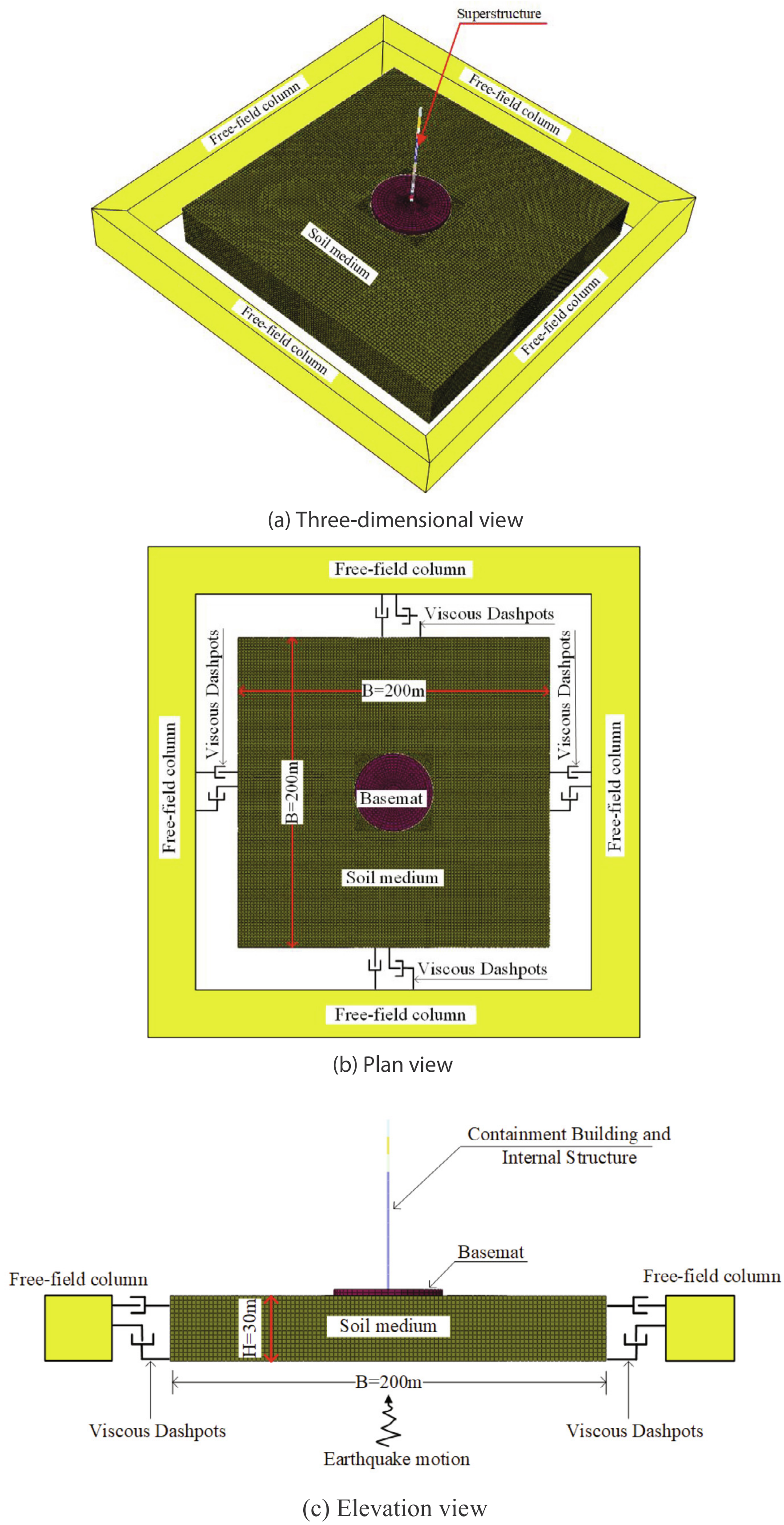

Fig. 4. Finite element model of soil-structure system.

Table 4
Material properties of the soil types.

Soil type	Young's modulus (kN/m^2)	Poisson's ratio	Mass density (t/m^3)	Material damping (%)	Friction Angle (degrees)	Cohesion yield (kN/m^2)
$S1$	$2.0x10^6$	0.30	2.0	5	30	190
$S2$	$5.0x10^5$	0.35	1.9	5	30	50
$S3$	$1.5x10^5$	0.35	1.9	5	30	50
$S4$	$7.5x10^4$	0.40	1.8	5	30	10

Table 5
Rayleigh damping coefficients for the soil medium.

Soil type	Mass-proportional coefficient (α)	Stiffness-proportional coefficient (β)
$S1$	2.4354	0.0008
$S2$	1.2260	0.0015
$S3$	0.6715	0.0028
$S4$	0.4790	0.0039

3. Earthquake motions

Three earthquake motions are used to consider the effect of earthquake frequency content in this study (Table 6). The frequency content of earthquakes are evaluated by using the ratio of peak ground acceleration (PGA) to peak ground velocity (PGV). As shown in Table 6, Loma Prieta, El Centro, and Cape Mendocino earthquakes are low, intermediate, and high frequency motions, respectively. The earthquake records are scaled in a way that the value of PGA reaches $0.4g$. The acceleration time histories and acceleration response spectra with 5% damping of three scaled earthquakes are plotted in Fig. 5. In this study, earthquake motions are applied at the bedrock of the soil medium.

4. Model verification

A code-to-code verification is applied in this study. The results from ABAQUS in the time domain are validated by using SASSI, a code in the frequency domain. Some studies have compared the results obtained in the time domain and frequency domain for seismic soil-structure interaction analysis [4,35]. Linear analyses are implemented in both ABAQUS and SASSI in this section. The soil type of $S4$ is considered for different earthquake records.

The responses at the top of the containment building, i.e. node 15 in Fig. 1(c) are obtained. Fig. 6(a)-(c) present both time history accelerations and acceleration response spectra for Loma Prieta, El Centro, and Cape Mendocino earthquakes, respectively. The results calculated by using ABAQUS and SASSI are almost identical. It indicates that the models of soil-structure interaction system in ABAQUS and SASSI are equivalent. The slight discrepancies can be explained due to the use of different damping formulations in the time and frequency domains. In the frequency domain, material damping is used, while Rayleigh damping is applied in the time domain.

5. Results and discussions

The results are discussed in terms of the acceleration response spectra at the top of the containment building, the maximum accelerations and maximum displacements along the height of the containment building. Three analysis cases are considered: linear analysis, nonlinear analysis with the bonded contact between the basemat and soil medium, and nonlinear analysis with the sliding contact between the basemat and soil medium.

5.1. Linear analysis

Fig. 7 shows the 5% damping acceleration response spectra at the top of the containment building for each soil type with different earthquake motions. In general, the acceleration values is decreased when the soil stiffness decreases for all ground motions. And, the fundamental frequency of the system is shifted for different soil types, for example, 3 (Hz) for $S1$ soil type and 1 (Hz) for $S4$ soil type. That can be explained by the increase of the flexibility of the system with the decrease of the soil stiffness. In other words, the fundamental frequency of the system is reduced in the soft soil medium because of the increase of radiation damping in the soil medium, which contributes to the total damping of the system. For soft soil ($S3$ and $S4$ soil types), Loma Prieta earthquake with low frequency content gives higher accelerations compared with El Centro with intermediate frequency content and Cape Mendocino with high frequency content. However, for the stiff soil ($S1$), an opposite trend occurs, i.e. the higher accelerations are found in Cape Mendocino earthquake with high frequency content. The reason for that phenomenon comes from the similar dynamic characteristics between the soft soil and low frequency earthquake, and also between the stiff soil and high frequency earthquake.

Maximum acceleration values along the height of the containment building are shown in Fig. 8. Now, the phenomenon as discussed for the acceleration response spectra is clearer. The maximum accelerations are higher in stiff soil media. Again, it can be explained by the decrease of the radiation damping in the stiff soil media. That leads to the higher accelerations. In the soft soil ($S3$ and $S4$), the values of maximum acceleration obtained from low frequency earthquake (Loma Prieta) are significantly higher than that in intermediate and high frequency earthquakes. For example, in $S4$ soil type, the maximum accelerations at the top of the containment building are $4.058g$, $1.728g$, and $0.518g$ for Loma Prieta, El Centro, and Cape Mendocino, respectively. It is worth noting that for Loma Prieta earthquake, the maximum acceleration values are similar for different soil types. Therefore, in terms of maximum acceleration, the influence of the soil-structure interaction is not great in low frequency earthquake as in intermediate and high frequency ones.

In terms of maximum displacement (Fig. 9), as expected, soft soil media experience the higher values. Again, the reason for that is due to the increase of the flexibility in the soft soil. Here, displacements are calculated as relative displacements with respect to the base of the

Table 6
Properties of earthquake ground motions.

Earthquake motion	Station	PGA (g)	PGV (m/s)	PGA/PGV	Frequency content
1989 Loma Prieta	Hollister – South & Pine	0.369	0.628	0.588	Low
1940 El Centro	El Centro, CA	0.319	0.335	0.954	Intermediate
1992 Cape Mendocino	Shelter Cove, CA	0.314	0.103	3.049	High

PGA: Peak ground acceleration; PGV: Peak ground velocity.

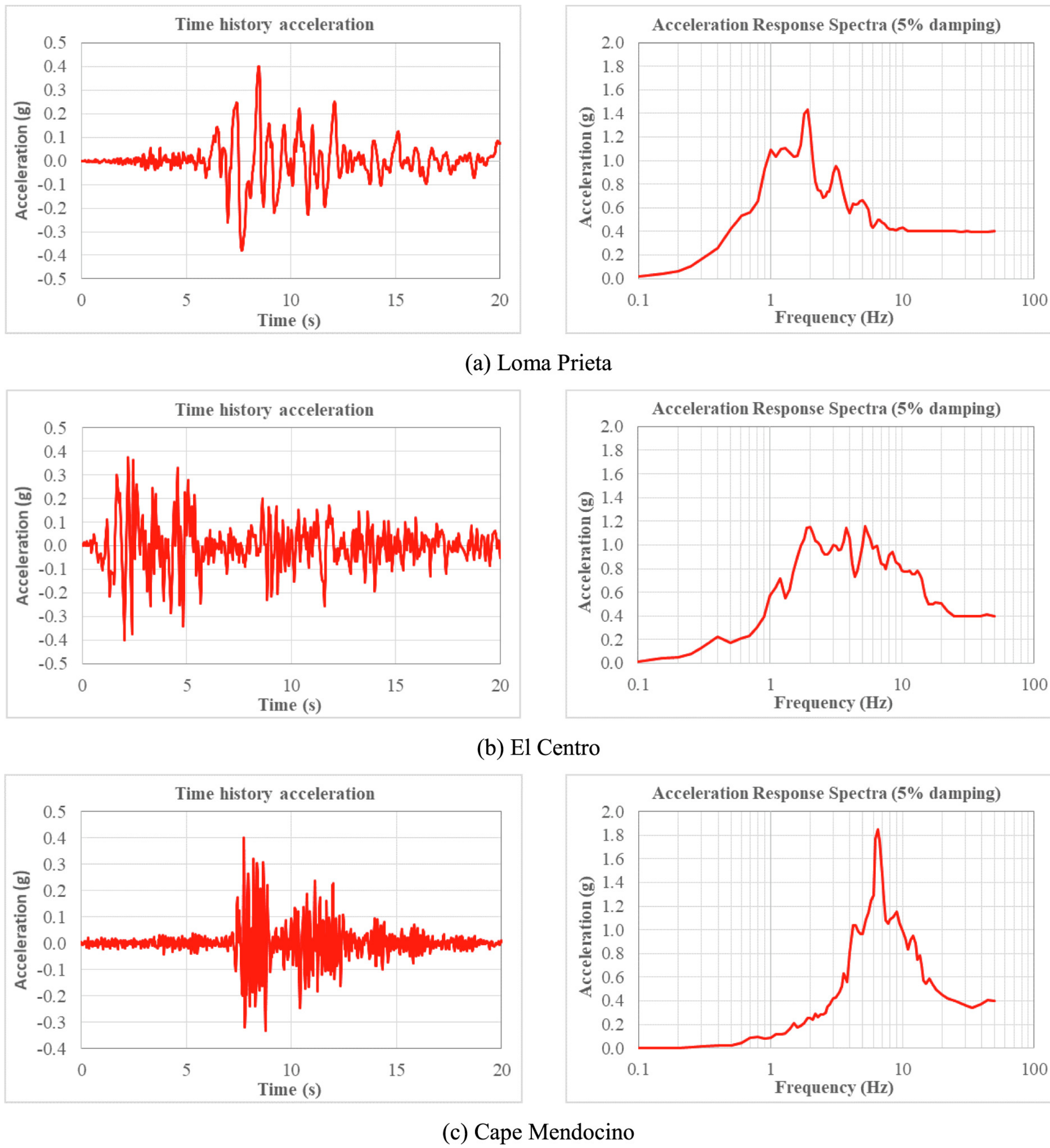

Fig. 5. Scaled earthquake motions.

superstructure. In most cases, the high frequency earthquake (Cape Mendocino) generates smaller maximum displacements, for instance, at the top of the containment building, 0.201m of maximum displacement obtained from Cape Mendocino compared with 0.542m in case of El Centro and 1.422m in case of Loma Prieta for the $S4$ soil type. If the soil stiffness increases the effect of earthquake frequency content on the maximum displacement is decreased. And, for $S1$ soil type, the differences between different earthquakes are negligible.

As a result, the effect of soil-structure interaction on the structural behavior depends on the earthquake frequency content and vice versa.

5.2. Nonlinear analysis with bonded contact between superstructure and soil medium

In this section, the system is analyzed with nonlinear material models. Here, nonlinearity is taken into account for both of soil medium and superstructure. Bonded contact is applied for the contact between the basemat and soil medium. To represent this type of contact, 'surface-to-surface' contact with 'no separation after contact' and 'frictionless' for tangential behavior is applied in ABAQUS. Fig. 10 presents the acceleration response spectra with 5% damping at the top of the containment building. It is easy to see that the acceleration values in the nonlinear analysis are significantly smaller than that in the linear analysis. The softening behavior in the nonlinear analysis is known as the main reason for those differences. Stiffness of the system is degraded through softening behavior. The trend is kept the same as in the linear analysis, i.e. higher accelerations for stiff soil media.

As shown in Fig. 10, the acceleration values between different ground motions for each soil type are closer than that in the linear analysis. And, the evaluation is strengthened in Fig. 11, which indicates the maximum acceleration values along the height of the containment building. Although the maximum accelerations are higher for stiff soil,

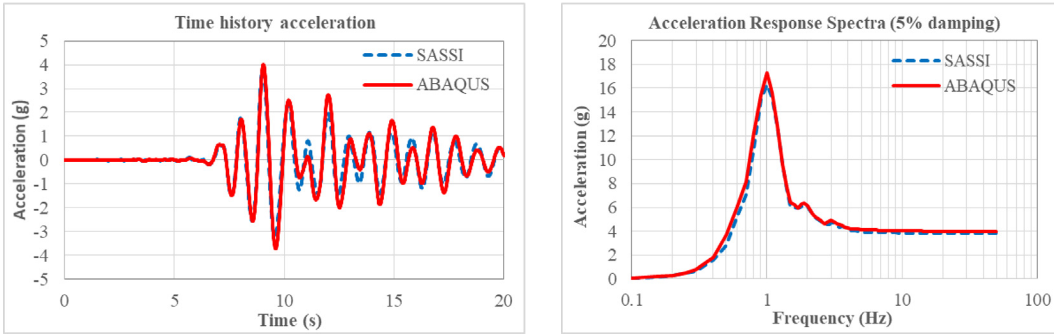

(a) Loma Prieta

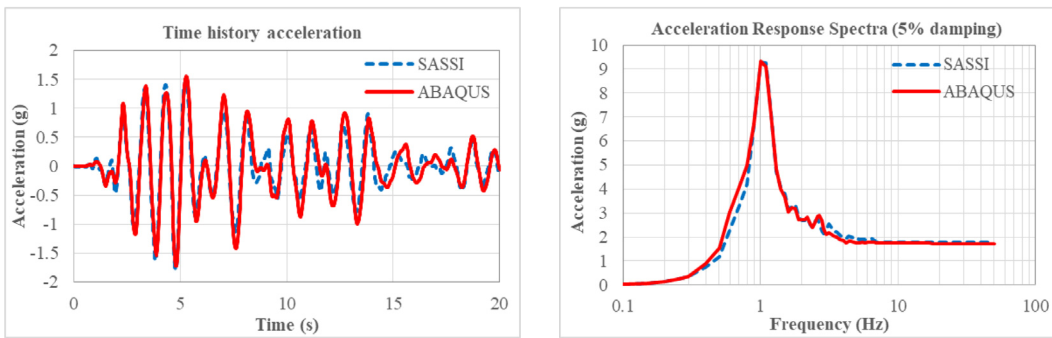

(b) El Centro

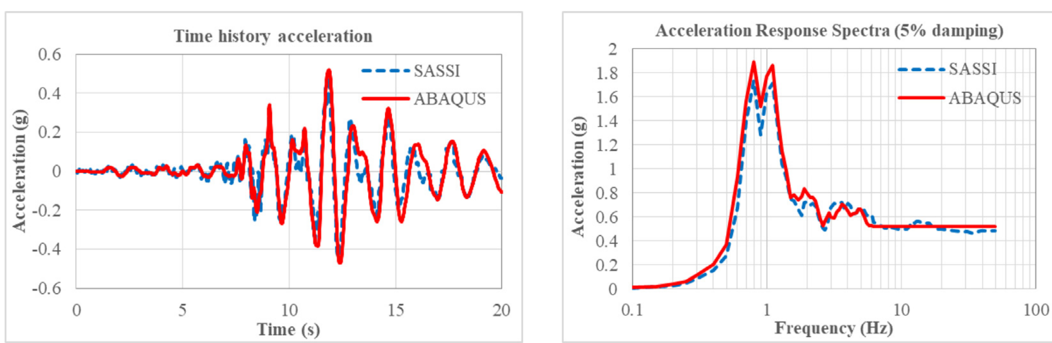

(c) Cape Mendocino

Fig. 6. Acceleration responses at the top of the containment building for $S4$ soil type.

the values for different earthquakes in each soil type are almost the same. Consequently, for the nonlinear analysis, the effect of the soil-structure interaction on the acceleration responses is more dominant than the effect of earthquake frequency content.

The maximum displacements along the height of the containment building are plotted in Fig. 12. The figure shows that the maximum displacement values in the nonlinear analysis are smaller than that in the linear analysis. This is expected because of more earthquake energy dissipation in the nonlinear soil medium. In general, the maximum displacement increases with the decrease of the frequency content of earthquakes for all soil types. For instance, in case of $S2$ soil type, there is a significant increase from $0.021m$ for high frequency earthquake (Cape Mendocino) to the value of $0.171m$ for Loma Prieta earthquake with low frequency earthquake.

5.3. Nonlinear analysis with sliding contact between superstructure and soil medium

Sliding contact between the basemat and the soil medium, which is associated with sliding and separation between structure and soil, is considered. The 'surface-to-surface' contact in ABAQUS with tangential and normal behavior is employed. The friction coefficient is calculated from the friction angle of the soil medium. With the friction angle (ϕ) of 30^0 for all soil types, the friction coefficient is determined as $tan\phi = 0.58$. The normal behavior is pressure-overclosure with hard contact. That allows any contact pressure can be transferred from one surface to another as long as they are in contact. And, the contact pressure decreases to zero when the surfaces are separated.

Figs. 13 and 14 present the acceleration response spectra at the top and maximum acceleration values along the height of the containment building, respectively. Except the soil type of $S1$, with the application of sliding contact, the acceleration values are kept almost unchanged compared with the bonded contact case. Hence, in terms of acceleration responses, sliding contact in the nonlinear analysis can be neglected in most of the cases.

Similar to the bonded contact nonlinear analysis, in the sliding case, the values of maximum displacement are higher for low frequency earthquake in most soil types (Fig. 15). For high frequency earthquake (Cape Mendocino), maximum displacements between two cases, i.e. bonded and sliding contacts, are similar for different soil types. For El Centro earthquake, sliding contact analysis experiences higher maximum displacements for all soil types compared with the bonded case. And, the phenomenon takes place for the soil types of $S1$ and $S4$ in case of Loma Prieta earthquake with low frequency content. That can be

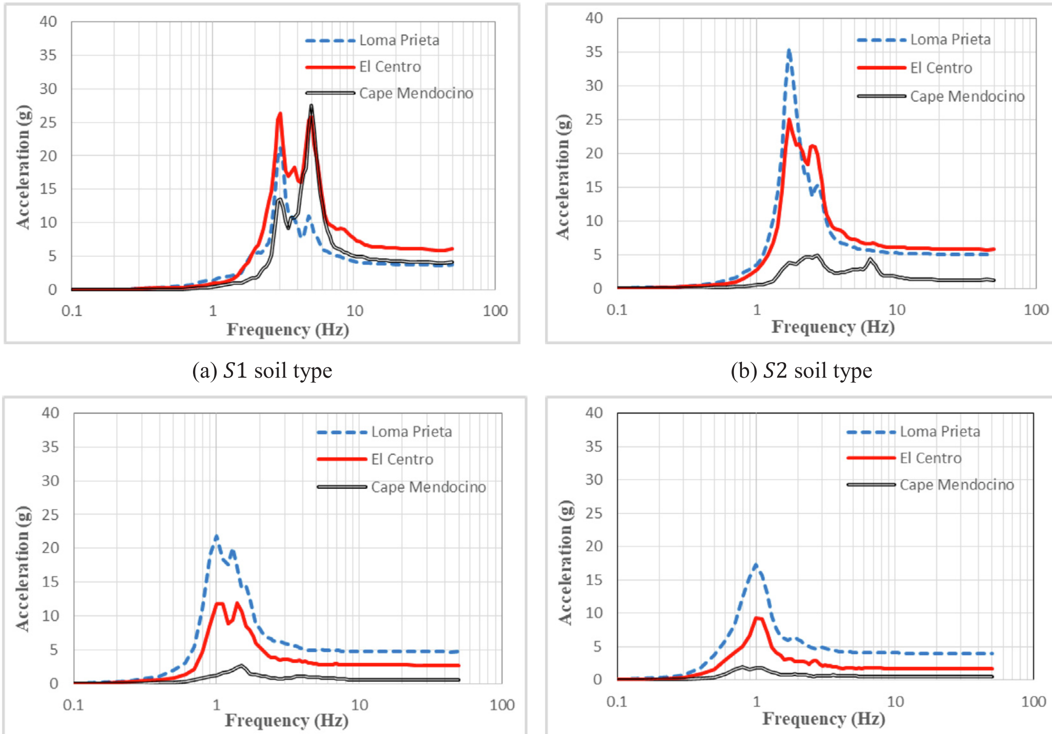

(a) $S1$ soil type

(b) $S2$ soil type

(c) $S3$ soil type

(d) $S4$ soil type

Fig. 7. Acceleration response spectra (5% damping) at the top of the containment building – Linear analysis.

explained from higher earthquake energy dissipation with the consideration of nonlinear contact between the structure and soil. And, it should be noted that the differences between displacements for different earthquakes are more significant than those in terms of acceleration. That can be explained by the softening effect in the nonlinear analyses, especially for soft soil. In this case, displacement response is more sensitive to the earthquake frequency content than acceleration response.

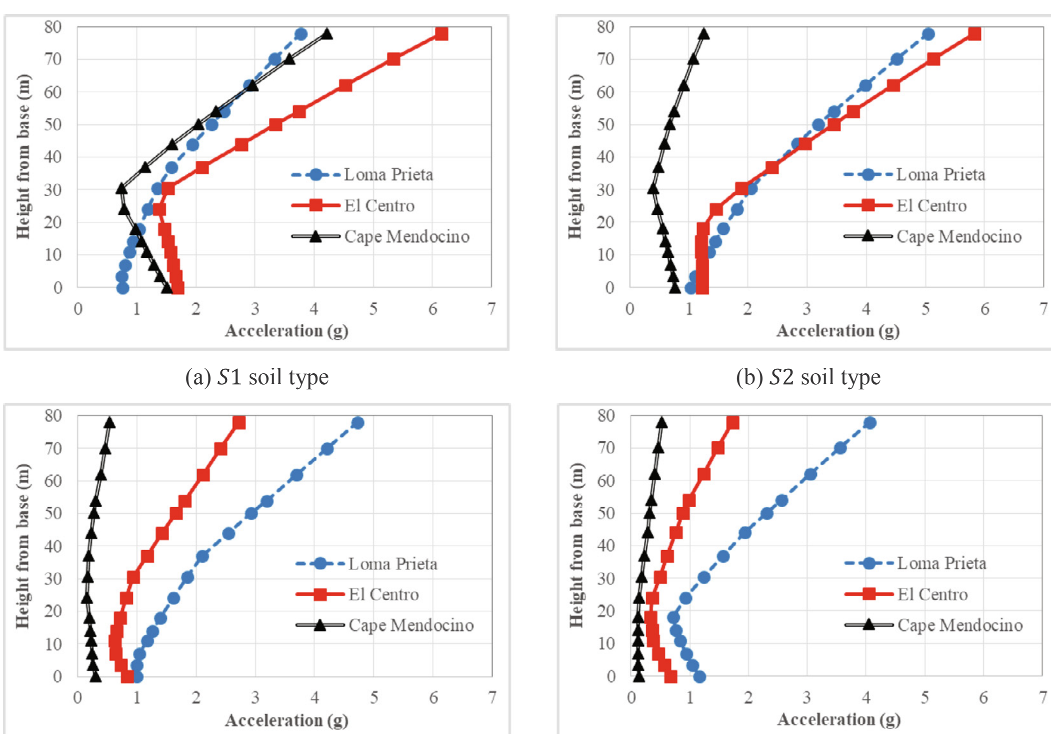

(a) $S1$ soil type

(b) $S2$ soil type

(c) $S3$ soil type

(d) $S4$ soil type

Fig. 8. Maximum accelerations along the height of the containment building – Linear analysis.

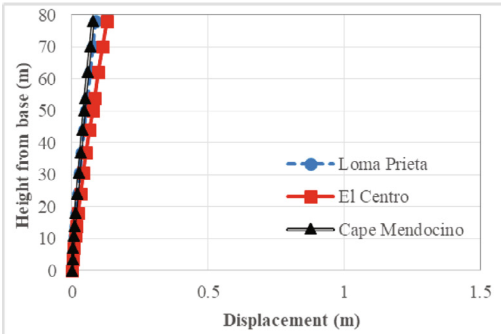

(a) $S1$ soil type

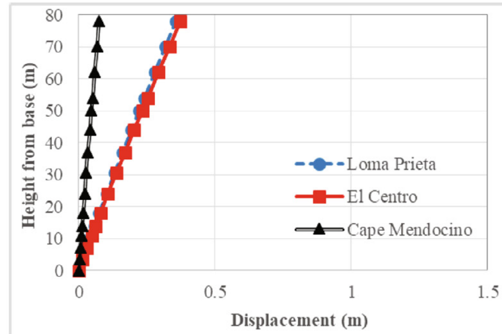

(b) $S2$ soil type

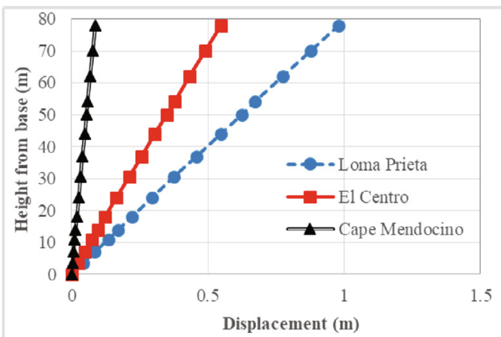

(c) $S3$ soil type

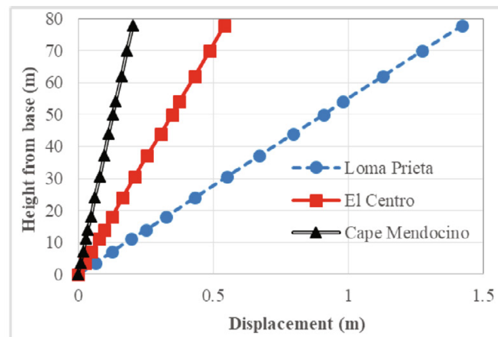

(d) $S4$ soil type

Fig. 9. Maximum displacements along the height of the containment building – Linear analysis.

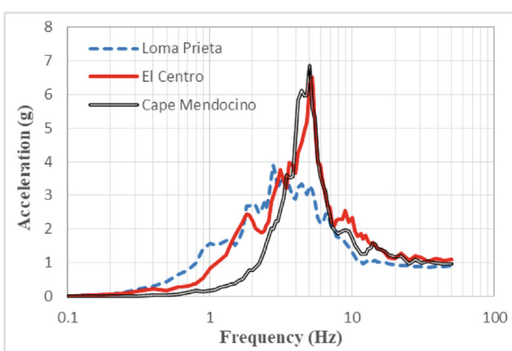

(a) $S1$ soil type

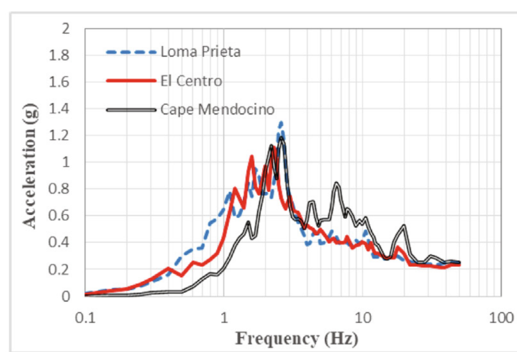

(b) $S2$ soil type

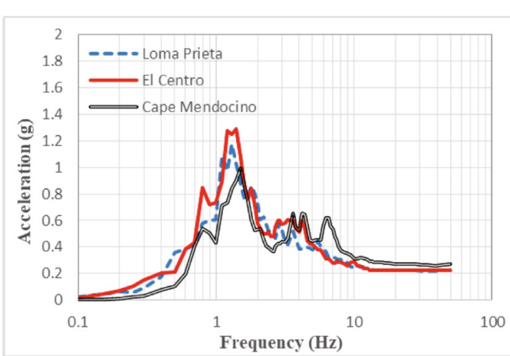

(c) $S3$ soil type

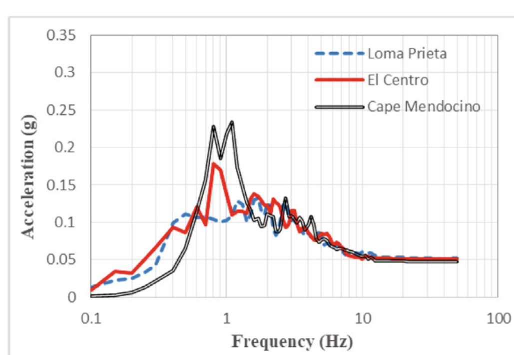

(d) $S4$ soil type

Fig. 10. Acceleration response spectra (5% damping) at the top of the containment building – Nonlinear analysis with bonded contact.

6. Conclusions

A three-dimensional seismic soil-structure interaction analysis of a nuclear reactor building is simulated to investigate the effects of soil-structure interaction and earthquake frequency content on the structural responses. Four types of soil with different properties and three types of earthquake motions with different frequencies are used. In order to absorb the spurious propagating waves in the soil model,

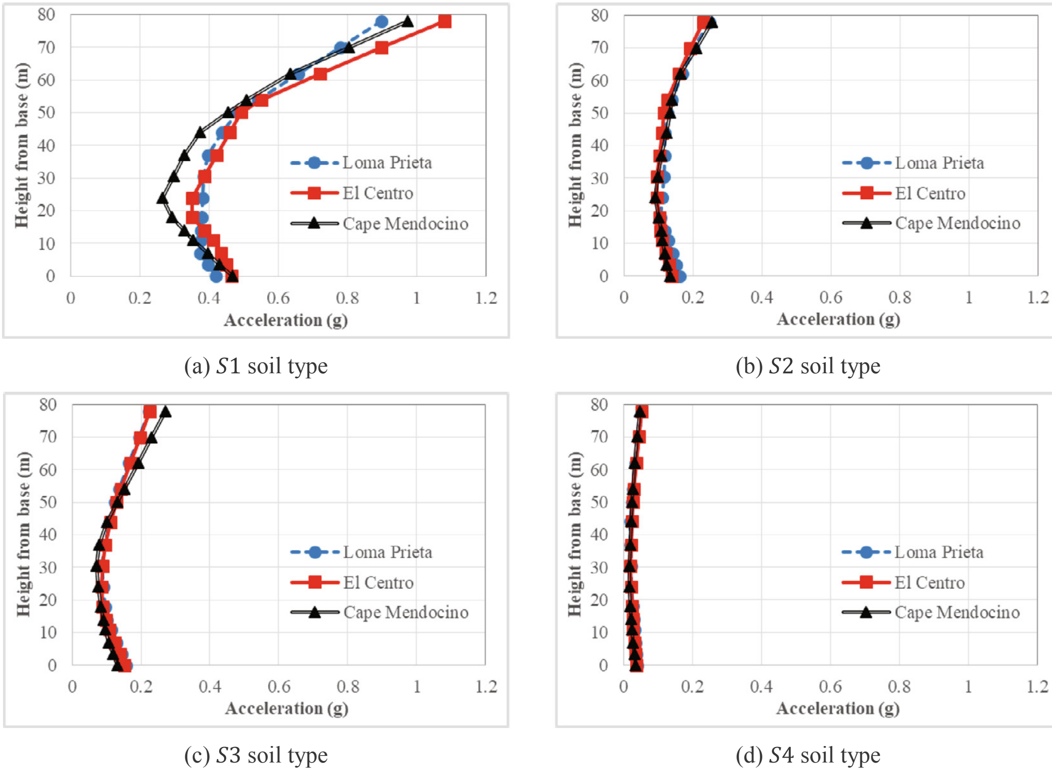

(a) $S1$ soil type

(b) $S2$ soil type

(c) $S3$ soil type

(d) $S4$ soil type

Fig. 11. Maximum accelerations along the height of the containment building – Nonlinear analysis with bonded contact.

viscous dashpots are applied along the soil boundaries. And, the free-field motion of the soil medium is simulated by using free-field columns. Analysis of three cases are presented, i.e. linear analysis; nonlinear analysis with the bonded contact between structure and soil; and nonlinear analysis with the sliding contact between structure and soil. The nonlinear material in analyses is taken into account by using concrete damaged plasticity and Drucker-Prager models for the concrete and soil materials, respectively. The numerical models are verified by adopting the code-to-code verification. The numerical results obtained from ABAQUS in the time domain are compared with that from

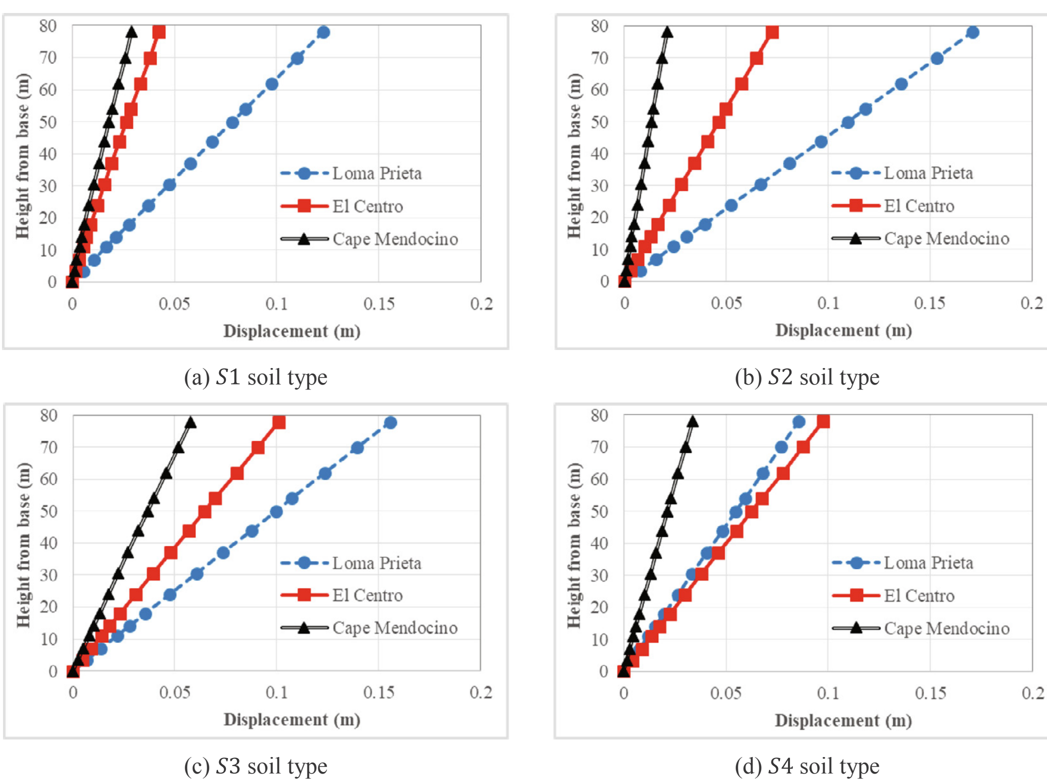

(a) $S1$ soil type

(b) $S2$ soil type

(c) $S3$ soil type

(d) $S4$ soil type

Fig. 12. Maximum displacements along the height of the containment building – Nonlinear analysis with bonded contact.

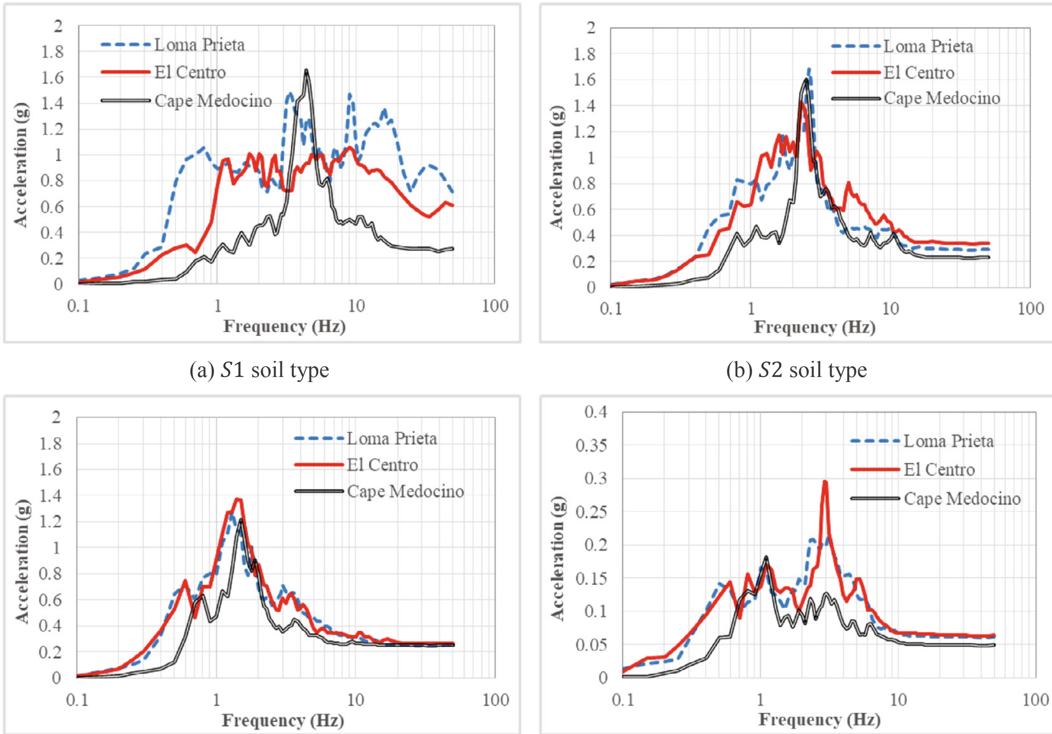

(a) $S1$ soil type

(b) $S2$ soil type

(c) $S3$ soil type

(d) $S4$ soil type

Fig. 13. Acceleration response spectra (5% damping) at the top of the containment building – Nonlinear sliding analysis.

SASSI, a code in the frequency domain. A good agreement between results from the two codes is observed.

The following conclusions can be drawn from the numerical results in this paper:

- The results show that the nuclear reactor responses are highly sensitive to both the soil-structure interaction and earthquake frequency content. The soil properties influence on the effect of earthquake frequency content on the behavior of the nuclear reactor building. Also, the earthquake frequency content is one of the

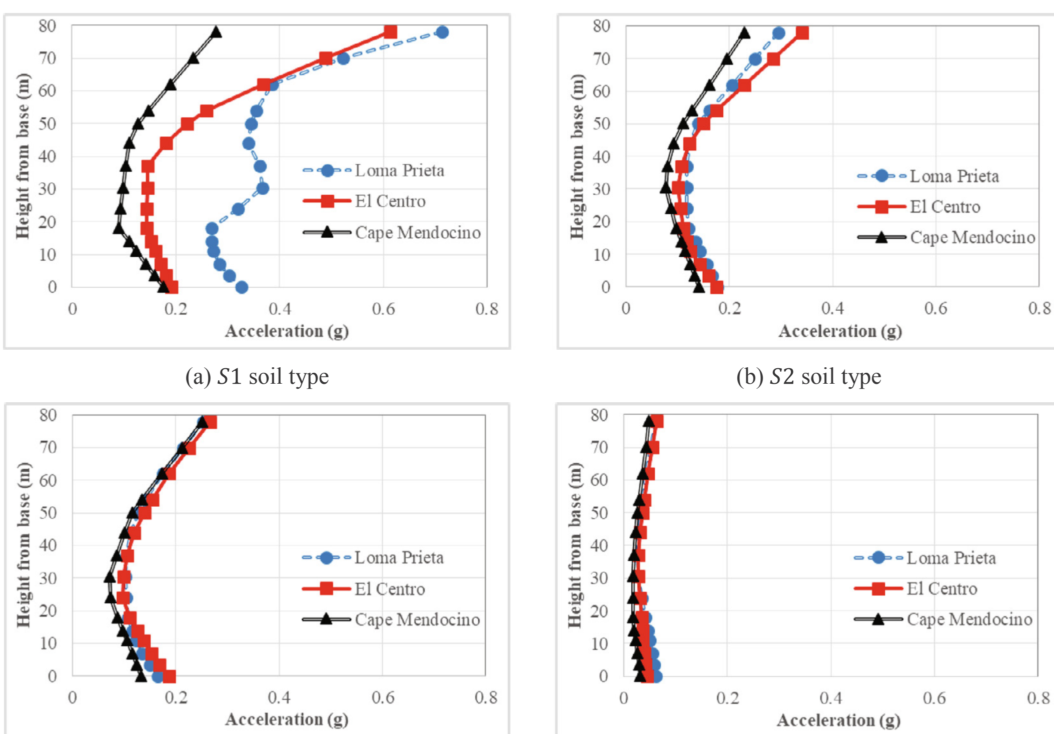

(a) $S1$ soil type

(b) $S2$ soil type

(c) $S3$ soil type

(d) $S4$ soil type

Fig. 14. Maximum accelerations along the height of the containment building – Nonlinear sliding analysis.

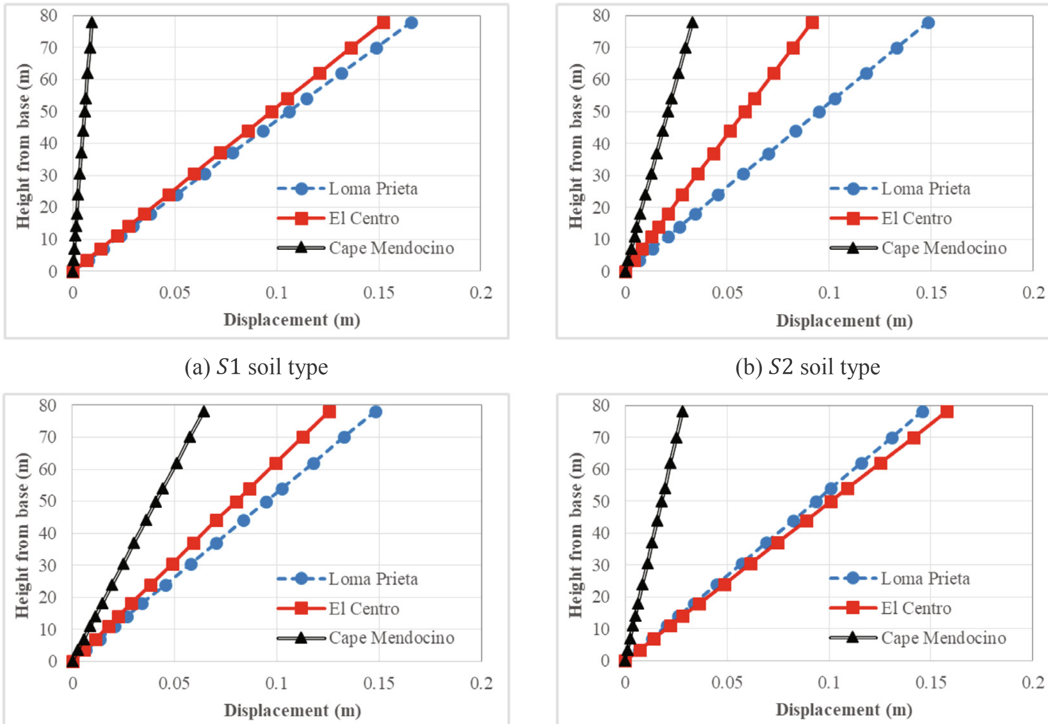

(a) $S1$ soil type

(b) $S2$ soil type

(c) $S3$ soil type

(d) $S4$ soil type

Fig. 15. Maximum displacements along the height of the containment building – Nonlinear sliding analysis.

factors determine the level of the effect of soil-structure interaction on the system. And, different kinds of analyses contribute different amount of the effects of soil-structure interaction and earthquake frequency content on the nuclear reactor performances. In order to fully evaluate the effects of soil-structure interaction and earthquake frequency content, both nonlinear material and nonlinear contact between structure and soil should be considered.

- Linear analyses generate the results including acceleration and displacement responses are significantly higher than nonlinear cases for all the soil types and earthquake motions. The consideration of the sliding contact in nonlinear analyses can be neglected in terms of acceleration responses in most of the cases.
- In most cases, the high frequency earthquake generates smaller maximum displacements in linear analyses. If the soil stiffness increases the effect of earthquake frequency content on the maximum displacement is decreased. And, for stiff soil type, the differences of maximum displacements between different earthquakes are negligible.
- In nonlinear analysis with bonded contact, although the maximum accelerations are higher for stiff soil, the values for different earthquakes in each soil type are almost the same. Consequently, the effect of the soil-structure interaction on the acceleration responses is more dominant than the effect of earthquake frequency content. Additionally, the maximum displacement increases with the decrease of the frequency content of earthquakes.

The research can be extended for the embedded foundation case. And, the simulation with the shell elements instead of using link elements is a promising research in the future.

Declaration of Competing Interest

The authors declare that they have no known competing financial interests or personal relationships that could have appeared to influence the work reported in this paper.

Acknowledgment

The National Research Foundation of Korea Grant funded by the Korean Government (NRF-2018R1A2B2005519) supported this work.

References

[1] Zhou Z, Wei X. Seismic soil-structure interaction analysis of isolated nuclear power plants in frequency domain. Shock Vib 2016;2016.
[2] Kumar S, Raychowdhury P, Gundlapalli P. Response analysis of a nuclear containment structure with nonlinear soil–structure interaction under bi-directional ground motion. Int J Adv Struct Eng (IJASE) 2015;7(2):211–21.
[3] Abell JA, et al. Earthquake soil-structure interaction of nuclear power plants, differences in response to 3-D, 3× 1-D, and 1-D excitations. Earthquake Eng Struct Dyn 2018;47(6):1478–95.
[4] Bolisetti C, Whittaker AS, Coleman JL. Linear and nonlinear soil-structure interaction analysis of buildings and safety-related nuclear structures. Soil Dyn Earthquake Eng 2018;107:218–33.
[5] Ostadan, F, Chen C, Lysmer J. SASSI2000—a system for analysis of soil–structure interaction. University of California, Berkeley, CA, USA; 2000.
[6] Abaqus, 6.14 Documentation, in Dassault Systemes Simulia Corporation; 2014.
[7] Lysmer J, Kuhlemeyer RL. Finite dynamic model for infinite media. J Eng Mech Div 1969;95(4):859–78.
[8] Berenger J-P. A perfectly matched layer for the absorption of electromagnetic waves. J Comput Phys 1994;114(2):185–200.
[9] Guddati MN, Tassoulas JL. Continued-fraction absorbing boundary conditions for the wave equation. J Comput Acoust 2000;8(01):139–56.
[10] Nguyen DV, Kim D. Perfectly matched discrete layers with analytical wavelengths for soil–structure interaction analysis. Int J Struct Stab Dyn 2018;18(09):1850103.
[11] Nguyen DV, et al. Seismic soil-structure interaction analysis of concrete gravity dam using perfectly matched discrete layers with analytical wavelengths. J Earthquake Eng 2019:1–22.
[12] Van Nguyen D, Kim D. Dynamic soil-structure interaction analysis in time domain based on a modified version of perfectly matched discrete layers. J Rock Mech Geotech Eng 2019.
[13] Kim DK, Yun CB. Time-domain soil–structure interaction analysis in two-dimensional medium based on analytical frequency-dependent infinite elements. Int J Numer Meth Eng 2000;47(7):1241–61.
[14] Kim DK, Yun CB. Earthquake response analysis in the time domain for 2D soil–-structure systems using analytical frequency-dependent infinite elements. Int J Numer Meth Eng 2003;58(12):1837–55.
[15] Wolf, J. Dynamic soil-structure interaction. Englewood Cliffs, NJ: Prentice Hall, Inc. ; 1985.
[16] Zienkiewicz, O., N. Bicanic, and F. Shen. Earthquake Input Definition and the

Trasmitting Boundary Conditions, in Advances in computational nonlinear mechanics. Springer. p. 109-138; 1989.
[17] McGuire RK. Seismic ground motion parameter relations. J Geotech Eng Div 1978;104(4):481–90.
[18] Rathje EM, et al. Empirical relationships for frequency content parameters of earthquake ground motions. Earthquake Spectra 2004;20(1):119–44.
[19] Newmark, N.M., W. Hall, and B. Mohraz. A study of vertical and horizontal earthquake spectra. Report WASH-1255, Directorate of Licensing, US Atomic Energy Commission; 1973.
[20] Tso W, Zhu T, Heidebrecht A. Engineering implication of ground motion A/V ratio. Soil Dyn Earthquake Eng 1992;11(3):133–44.
[21] Kianoush M, Ghaemmaghami A. The effect of earthquake frequency content on the seismic behavior of concrete rectangular liquid tanks using the finite element method incorporating soil–structure interaction. Eng Struct 2011;33(7):2186–200.
[22] Cakir T. Evaluation of the effect of earthquake frequency content on seismic behavior of cantilever retaining wall including soil–structure interaction. Soil Dyn Earthquake Eng 2013;45:96–111.
[23] Lee H, et al. Simplified model and seismic response of integrated nuclear containment system based on frequency adaptive lumped-mass stick modeling approach. KSCE J Civ Eng 2015;19(6):1757–66.
[24] Ali SB, Kim D. Wavelet analysis of soil-structure interaction effects on seismic responses of base-isolated nuclear power plants. Earthquakes Struct 2017;13(6):561–72.
[25] Bolisetti C, Whittaker A. Seismic structure–soil–structure interaction in nuclear power plant structures. Trans SMiRT 2011;21:6–11.
[26] Bolisetti C, Coleman J. Advanced Seismic Soil Structure Modeling. US Department of Energy Office of Nuclear Energy 2015.
[27] Chopra, A.K. Dynamics of structures: theory and applications to earthquake engineering. Vol. 3. Pearson/Prentice Hall Upper Saddle River, NJ; 2007.
[28] Rayhani M, El Naggar MH. Numerical modeling of seismic response of rigid foundation on soft soil. Int J Geomech 2008;8(6):336–46.
[29] Bardet, J.-P. Experimental soil mechanics. Prentice Hall Upper Saddle River, NJ; 1997.
[30] Coduto, D.P., W.A. Kitch, and M.-c.R. Yeung. Foundation design: principles and practices. Vol. 2. Prentice Hall Upper Saddle River; 2001.
[31] Alejano LR, Bobet A. Drucker-Prager Criterion. Rock Mech Rock Eng 2012;45(6):995–9.
[32] Bui HH, et al. Lagrangian meshfree particles method (SPH) for large deformation and failure flows of geomaterial using elastic–plastic soil constitutive model. Int J Numer Anal Meth Geomech 2008;32(12):1537–70.
[33] Chen, W-F, Baladi GY. Soil plasticity: theory and implementation. Vol. 38. Elsevier; 1985.
[34] Rowe, R.K. Geotechnical and geoenvironmental engineering handbook. Springer Science & Business Media; 2012.
[35] Xu, J., et al., ASSESSMENT OF SEISMIC ANALYSIS METHODOLOGIES FOR DEEPLY EMBEDDED NPP STRUCTURES. 2005, BROOKHAVEN NATIONAL LABORATORY (US).